

**CHAPTER VII**  
**SURFACE ACTIVITY OF KL AND Rh/KL CATALYSTS**  
**IN WASTE TIRE PYROLYSIS**

**7.1 Abstract**

A variety of catalysts have been used on the attempts to improve the quality of tire-derived oil. Usually, most research articles reported the impacts of catalysts on the quality and quantity of products, but not so many of them revealed the surface activity or changes of hydrocarbon species on the surface. In our previous work, a Rh/KL catalyst was tested for waste tire pyrolysis, and it was preliminarily found that the catalyst significantly decreased the yield of di-aromatics (DAHs), poly-aromatics (PAHs), and polar-aromatics (PPAHs) in conjunction with a significant increase in mono-aromatics (MAHs). Since no research has been done to investigate the surface activity of KL and Rh/KL catalysts, the objective of this study was thus to examine and reveal the change in species of components in tire-derived oil over these catalysts. Especially, the significant increase of mono-aromatics in relation with the changes in di-, poly-, and polar-aromatics was examined and revealed. GCxGC / TOF-MS and HSQC-NMR were employed to analyze and verify hydrocarbon compounds in the oils, which were used to examine the activity on the surface of KL and Rh/KL. As a result, the KL catalyst can provide hydrogenation of C11- and C12-alkylbenzenes; moreover, it can enhance the cracking ability of C13- and C14-indenes. The surface activity of rhodium over KL catalyst was investigated, and found that the yield of C11-alkenylbenzenes increased in conjunction with decrease in C11-alkylbenzenes due to dehydrogenation, whereas the yield of C12-alkylbenzenes did not change; however, rhodium exhibited the ring opening ability on cyclohexylbenzene via multiplet mechanism. Furthermore, the dramatically increase of C12-DAHs (mostly, 2-ethylnaphthalene) was attributed to C12-tetralins (mostly, 2-ethyltetralins). Therefore, it can be concluded that rhodium over KL catalyst provided dehydrogenation and ring opening activities.

Keywords: Zeolite; Rh/KL; KL; Tyre pyrolysis; GC × GC / TOF-MS; HSQC-NMR

## 7.2 Introduction

The most commonly-found hydrocarbon compounds in the tire-derived oils (TDOs) are poly- and polar-aromatics (Williams *et al.*, 1990). Tire-derived oil generally consists of naphthene, fluorene, phenanthrene, pyrene. These chemicals may give rise to toxic and corrosive SO<sub>x</sub> in the exhaust stream of combustion (Williams and Nazzal, 1995). Recently, hydrocarbon compounds in a TDO have been categorized into seven groups according to their structure; that were, saturated hydrocarbons (SATs), olefins (OLEs), terpenes (TERs), mono-aromatics (MAHs), di-aromatics (DAHs), poly-aromatics (PAHs), and polar-aromatics (PPAHs) (Pithakratanayothin and Jitkarnka, 2014). Moreover, since MAHs are the majority in the TDO; then, they were also classified into two main classes; that are, mono-aromatics with saturated substituents (MAHs-SS) and mono-aromatics with unsaturated substituents (MAHs-US). The hydrocarbon compounds in MAHs-SS were also classified into three species; that are, benzene and alkylbenzenes, tetralins, and indanes whereas the hydrocarbon compounds in MAHs-US were classified into two species; that are, indenenes and alkenylbenzenes. Besides a high sulfur content, the main problems of aromatics, especially poly-aromatics in a TDO are that they are of low product value, and are carcinogenic and mutagenic. Therefore, a tire-derived oil needs hydrogenation and desulfurization to improve the quality before use as chemical feedstock (Williams and Besler, 1995).

A basic catalyst that has a K<sup>+</sup> as a cation such as potassium tert-butoxide (K<sup>+</sup>(CH<sub>3</sub>)<sub>3</sub>CO<sup>-</sup>) and K/Al<sub>2</sub>O<sub>3</sub> can provide both hydrogenation and aromatization activities. Stapp and Kleinschmidt (1965) studied the isomerization of cyclooctadienes to cis-Biscyclo[3.3.0]oct-2-ene, and reported that potassium tert-butoxide can hydrogenate linear dienes, like 1,5-hexadiene, to hexane. Moreover, Slaugh (1967) studied metal hydrides as hydrogenation and isomerization catalysts, and found that potassium hydride (KH) appeared to be several hundred times more active than sodium hydride. In addition, Slaugh (1968) studied the hydrogenation of

benzene to phenylcyclohexane using supported alkali metal catalysts, and found that the catalytic properties of alkali metals could be changed drastically by depositing them on certain supports. Furthermore, Friedman *et al.* (1971) found that alkali metals and alkali metal alloys can be used as catalysts for the hydrogenation of poly-aromatic hydrocarbons to products containing an isolate aromatic ring. In addition, a basic catalyst can also provide aromatization of hydrocarbon compounds. Pines and Eschinazi (1955) studied sodium-catalyzed double bonds migration and dehydrogenation of *d*-limonene and phellandrene, and found that the base catalyst can aromatize *d*-limonene to *p*-cymene. Moreover, Brown (1973) revealed potassium hydride with amine can provide aromatization of *d*-limonene to *p*-cymene at room temperature. In addition, a basic catalyst can also provide aromatization on the terpene hydrocarbon compounds such as *d*-limonene and 3-carene as well. A KL zeolite is a basic solid catalyst that contains  $K^+$  as a cation. It has basic property and one dimensional channel of 12-membered rings with a pore size of 0.71 nm (Sato *et al.*, 1999). KL has been employed as a support of Ru for the hydrogenation of unsaturated aldehyde (Álvarez-Rodríguez *et al.*, 2005). Azzam *et al.* (2010) studied the aromatization of hexane over Pt/KL catalyst, and they found that L-zeolite channels inhibited the coke formation and catalyst deactivation.

Rhodium was found to be one of the most active noble metal that higher yield in hydrogenation and the ring opening of naphthalene than Pt and Ir for diesel upgrading (Jacquin *et al.*, 2003). Nurunnabi *et al.* (2006) reported that the addition of 0.035% Rh on NiO-MgO made it the most effective catalyst to improve catalytic activity and inhibit carbon deposition in methane steam reforming. Jacquin *et al.* (2008) found that bimetallic PdRh showed activity and selectivity in hydrogenation and the ring opening of polyaromatic compounds. Several research articles in waste tire pyrolysis reported the uses of many catalysts to improve the quality of tire-derived oil. As in our previous work, Pinket (2010) studied the 1%Rh/KL for waste tire pyrolysis, and found that the Rh/KL catalyst significantly decreased the yield of di-aromatics (DAHs), poly-aromatics (PAHs), and polar-aromatics (PPAHs) in conjunction with a significant increase in mono-aromatics (MAHs). However, no detail on chemicals in MAHs, DAHs, PAHs, and PPAHs was reported, and the

surface activity, or the relative changes of hydrocarbons in the oil, on the surface of KL and Rh/KL was not explained clearly.

The study on the surface activity of the catalyst is very important for a researcher who wants to develop the catalyst that can provide a specific reaction. Moreover, mono-aromatics in the range of C6 – C8 are important petrochemicals that could possibly be produced in a TDO by using a selective catalyst. Since the Rh/KL catalyst was found to significantly enhance the content of mono-aromatic compounds in TDOs, the surface activity on the KL and Rh/KL was studied. The changes of chemical components in tire-derived oils were revealed by using a comprehensive 2D gas chromatograph with time-of-flight mass spectrometry (GC × GC- TOF/MS), which were categorized into seven groups; that are, saturated hydrocarbons (SATs), olefin hydrocarbons (OLEs), terpene hydrocarbons (TERs), mono-aromatic hydrocarbons (MAHs), di-aromatic hydrocarbons (DAHs), poly-aromatic hydrocarbons (PAHs), and polar-aromatic hydrocarbon (PPAHs). The changes of chemical components abundantly found in each group were confirmed by using the Two-dimension Heteronuclear Single-Quantum Correlation-Nuclear Magnetic Resonance (HSQC-NMR) technique.

### **7.3 Experimental**

#### **7.3.1 Catalyst Preparation**

The zeolite, Linde Type L (LTL, K-form, Si:Al = 3) supplied by the TOSOH Company (Singapore) was first calcined in air at 500 °C with the heating rate of 5 °C min<sup>-1</sup> for 3 hours. Then, the KL catalyst was loaded with Rh using the incipient wetness impregnation technique to obtain 1 %wt Rh-supported catalyst. The catalyst was next reduced at 400 °C for 3 hours. After that, the KL and Rh/KL were pelletized, ground, and then sieved to a specific particle size range of 400-425 μm before use.

### 7.3.2 Pyrolysis of Waste Tire

A used passenger tire tread, Bridgestone TURANZA GR-80, was shredded and sieved to a size range of 8-18 mesh. The tire pyrolysis experiments were conducted using the same pyrolysis system as in (Dũng *et al.*, 2009). The tire sample was pyrolyzed in the reactor where the temperature was ramped from room temperature to the final temperature of 500°C with the ramping rate of 10 °C min<sup>-1</sup>, and kept at the final temperature for one hour to ensure the total conversion of tire. 7 grams of the KL and 1% Rh/KL catalysts were packed and heated at 350 °C in the catalytic zone. A 25 ml min<sup>-1</sup> nitrogen was used to purge the reactor before the experiment and to carry the product out of the reactor. The obtained product was passed through the ice-salt condensing system containing two consecutive containers in order to separate the liquid product from incondensable compounds. After the experiment, the solid and liquid were weighed to determine the product distribution. The amount of gas was calculated from mass balance. Only the oil was brought to analysis in this study. It was first dissolved in n-pentane with the ratio of 40:1 (n-pentane:oil) to separate asphaltene. The clear solution after filtration is called maltene.

### 7.3.3 Analysis Using GC × GC – TOF/MS

The GC × GC–TOF/MS system was composed of an Agilent gas chromatograph 7890 (Agilent Technologies, Palo Alto, CA, USA), a thermal modulator, and a Pegasus® 4D TOF-MS (LECO, St. Joseph, MI, USA). The GC was installed with two columns: the first column was a non-polar Rtx 5 silms® (30m x 0.25 mm i.d. x 0.25 µm film thickness), and the second column a Rxi®-17 ms (1.10 m x 0.10 mm i.d. x 0.10 µm film thickness). Both columns were made by Thames Restek (Sounderton, UK). The main GC oven was operated from at 50 °C with 2 minute holding at the beginning and then ramped to 310 °C at 5 °C min<sup>-1</sup> with 10 minute holding at 310 °C, and the secondary oven was operated at 60 °C held for 2 minutes at the beginning and ramped to 320 °C at 5 °C min<sup>-1</sup> with 10 minute holding at the final temperature. One µl of the 10 mg/ml maltenes in carbondisulfide (CS<sub>2</sub>) was injected via a spiltless injector at 250 °C using He as the carrier and a constant

column flow rate of 1.0 ml/min. The modulator was operated under modulation timing of 4-s cycle time and 0.5-s holding time in the release position. The nitrogen cryogen coolant maintained the temperature of the modulation trap to at least 30 °C. A Pegasus 4D® TOF/MS instrument was used to acquire mass spectral data, using -70 V electron impact ionization. The ion source temperature was set at 250 °C. The detector voltage was set at 1600 V. The transfer line temperature was 250 °C. The mass range collected was from 35 to 500 m/z, with 100 spectra/s transferred to the data station. The data processing was set S/N value of 10, match required to combine 500, and dt that was used to calculate the percentage area. Data were recorded and analyzed using the LECO ChromaTOF® software. The NIST library provided with the instrument was used for spectral searching. The analysis was repeated for 3 times. The criteria used for identification hydrocarbon species were the area percentage that is higher than 0.1 % and matched peaks that were more than 750.

#### 7.3.4 Analysis using HSQC-NMR

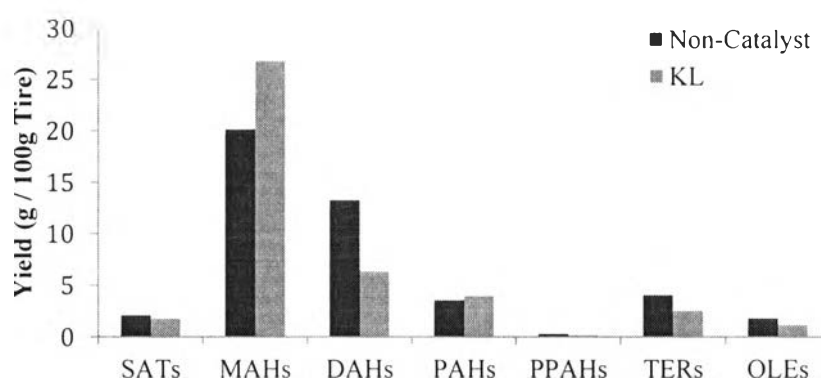
NMR is a powerful tool that can reveal the environment of an atom in a organic hydrocarbon molecule. Besides qualitative information, NMR can provide valuable quantitative information about a sample. As the complexity of a sample increases, the analysis can be complicated by the spectra overlapped each other. In fact, the limitations of 1D NMR can be overcome by using modern two-dimensional (2D) NMR techniques. Two-dimension Heteronuclear Single-Quantum Correlation-Nuclear Magnetic Resonance (HSQC-NMR) has been successfully used to analyze pyrolysis oil from kraft lignin (Ben and Ragauskas, 2011). All NMR spectra were recorded using a VARIN INOVA 500 MHz spectrometer at 32 °C in deuterated ( $\text{CDCl}_3-d$ ) chloroform as the solvent. 70 mg of maltenes from the non-catalyst, KL and 1%Rh/KL batches was dissolved in 0.5 mL of  $\text{CDCl}_3-d$ . 2D HSQC-NMR spectra were recorded by employing a standard VARIAN pulse sequence “s2pul (gHSQC)” with 90° pulse, 3.0 s acquisition time, 3.0 s relax delay,  $^1J_{C-H}$  145 Hz, 48 scans, and the spectral widths were 8000 and 32000 Hz for the  $^1\text{H}$  and  $^{13}\text{C}$  dimensions, respectively. The central solvent ( $\text{CDCl}_3$ ) peak was used as an internal chemical shift reference point ( $\delta\text{C}/\delta\text{H}$  77.2/7.26) (David *et al.*, 2008). Heteronuclear single-

quantum coherence (HSQC) data processing and plots were carried out using the default processing template and automatic phase and baseline correction of MestReNova, version 6.0.1, software. The analysis was repeated for 7 times.

## 7.4 Results and Discussion

### 7.4.1 Surface Activity of KL Catalyst

#### 7.4.1.1 Changes of Components in TDO with Using KL



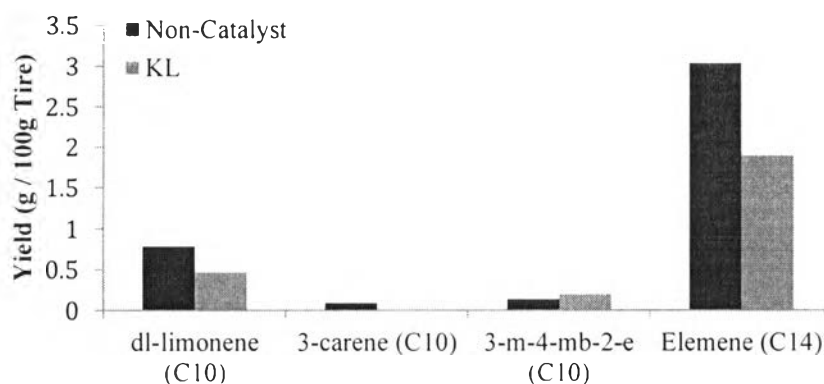
**Figure 7.1** Yield of hydrocarbon species in tire-derive oils from non-catalyst and KL batches.

Figure 7.1 shows the changes of products components in the tire-derived oil with using KL catalyst, and it was found that the KL catalyst decreases the yields of DAHs and TERs whereas the yield of MAHs significantly increases. Moreover, the yields of the yields of SATs, PAHs, PPAHs, and OLEs do not significantly change. Hence, the surface activity of KL catalyst can be revealed and explained by analyzing the details of changes of hydrocarbon species in DAHs, TERs and MAHs groups.

#### (a) Changes of Hydrocarbon Species in TERs and DAHs

Dominant compounds in the C<sub>10</sub>-TERs group are d-limonene ( $m/z = 136.125$ ), 3-carene ( $m/z = 136.125$ ) and 3-methyl-4-methylenebicyclo[3.2.1]oct-2-ene (3-m-4-mb-2-e) ( $m/z = 136.125$ )

(Pithakratanayothin and Jitkarnka, 2014). Figure 7.2 illustrates that the yields of C10-TERs; that are, d-limonene, 3-carene, and 3-methyl-4-methyleneBicyclo[3.2.1]oct-2-ene (3-m-4-mb-2-e), and C14-TERs (elemene). The yields of C10-TERs do not significantly change, but that of the C14 significantly decreases with using KL catalyst.



**Figure 7.2** Yield of hydrocarbon species in TERs.

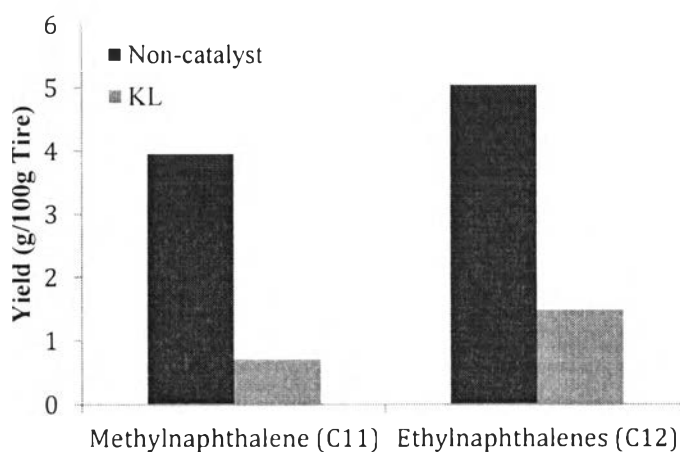


**Figure 7.3** Yield of hydrocarbon species in DAHs.

DAHs in TDOs are composed of hydrocarbons starting at C10 to C14, which mostly are naphthalene and alkylnaphthalenes (Pithakratanayothin and Jitkarnka, 2014). The hydrocarbon species in DAHs, found changed insignificantly upon the use of KL are methylnaphthalene(C11) and



ethylnaphthalene (C12). Figure 7.3 shows that the yields of C11- and C12-DAHs significantly decrease with using KL catalyst.

(b) *Changes of Hydrocarbon Species in MAHs*

According to Figure 7.1, the significant increments of MAHs are observed with using the KL catalyst; therefore, the changes of compounds in MAHs are then examined in details. Figure 7.4 shows the changes of hydrocarbon species in the MAHs group. It can be seen that alkenylbenzenes and indenenes significantly decrease; whereas alkylbenzenes and tetralins dramatically increase. The details on changes of each species based on carbon number were examined to investigate the changes of mono-aromatic compounds on these surface of KL catalyst. It is found that the yields of alkylbenzenes with carbon numbers (C10, C11, and C12) increase (Figure 7.5a) whereas only the yield of C12-tetralins dramatically increases (Figure 7.5b) with using KL catalyst. Moreover, the yields of C11- and C12-alkenylbenzenes decrease with using KL catalyst (Figure 7.5c). Indenenes range from C11-C14; however, only C13- and C14-indenenes are found to decrease with using KL catalyst (Figure 7.5d).

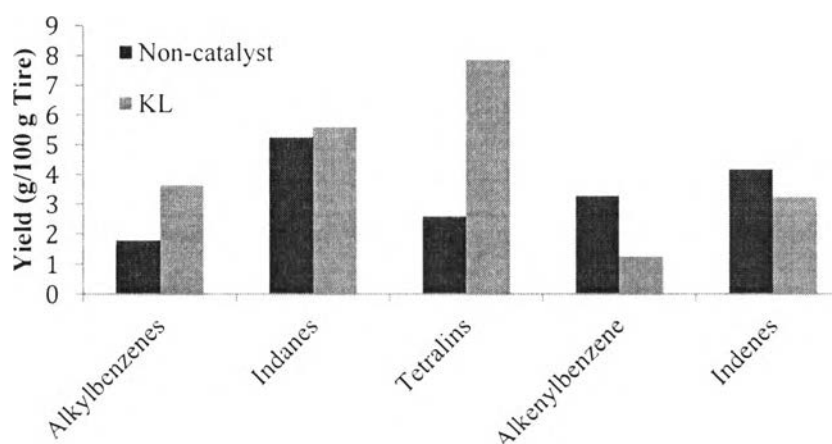


**Figure 7.4** Yield of hydrocarbon species in MAHs.

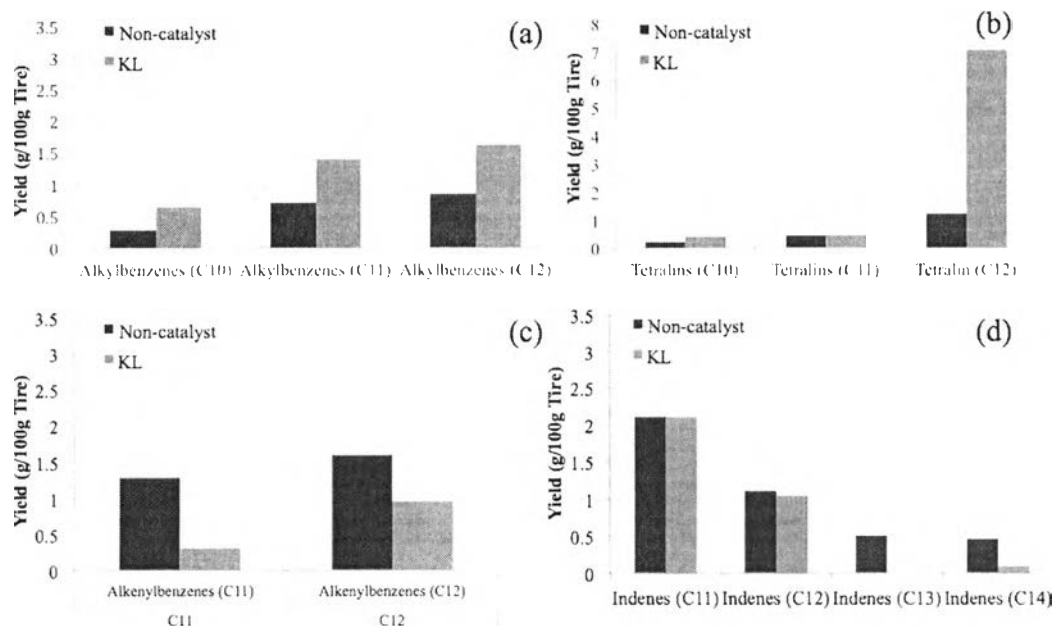


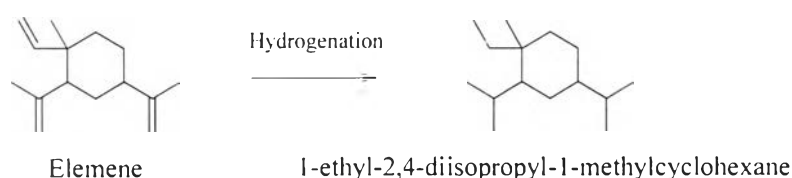
**Figure 7.5** Yields of (a) alkylbenzenes, (b) tetralins, (c) alkenylbenzenes, and (d) indenenes in each carbon number.

#### 7.4.1.2 Possible reactions on KL catalyst

Based on the results, it is able to draw the diagram of possible reactions taking place on the surface of KL catalyst as shown in Figure 7.6. Since it was found that the yields of SATs, PAHs, PPAHs, and OLEs groups did not significantly change (see Figure 7.1), and the objective of this work was aimed at explain how mono-aromatic compounds were produced tremendously with using KL catalyst; therefore, only the significant changes of MAHs and DAHs are taken into consideration, which can be divided into two types; that are, the conversions within MAHs group and between two groups (the conversion of DAHs to MAHs) as depicted in Figure 7.6.

The changes within MAHs occur from the conversion of C12-alkenylbenzenes to C12-alkylbenzenes and the conversion of C11-alkenylbenzenes to C11-alkylbenzenes (Figure 7.6). The changes from DAHs to MAHs would be resulted from the conversion of C12-DAHs to C12-tetralins (Figures 7.3 and 7.5b). Furthermore, the changes of TERs (C14) and indenenes (C13 and C14) could be

explained by taking consideration on a substance called “elemene” (a C14-terpene), whose the molecular structure is shown in Figure 7.7(a). It can be seen that elemene could have been converted to alkenylbenzenes or alkylbenzenes by either dehydrogenation or aromatization, but the results show no existences of C14-alkylbenzenes and C14-alkenylbenzenes.



Likewise, C13- and C14-indenes whose structure are shown in Figure 7.7 (b) and (c) respectively, could have been converted to C13- and C14-indanes by hydrogenation, but the results show that the yields of indanes do not change with using KL catalyst. Thus, it can be concluded that C14-elemene in TERs and C13- and C14-indenes would have rather cracked by the KL catalyst.

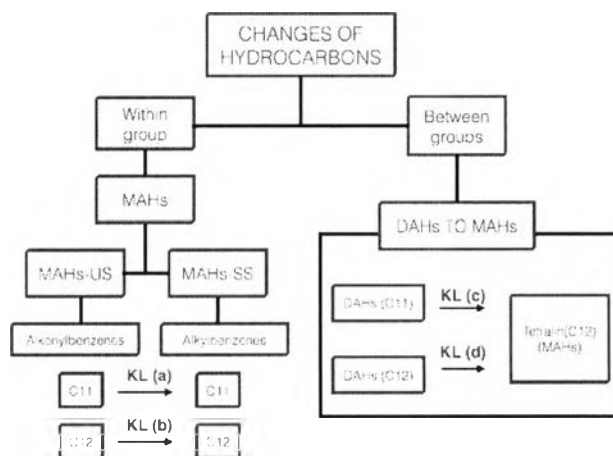


**Figure 7.6** Possible reactions on KL catalyst.

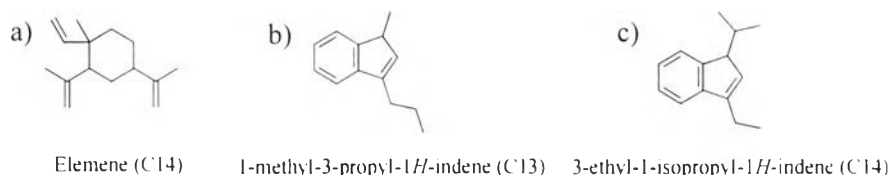


**Figure 7.7** Chemical structures of (a) a C14-terpene, (b) a C13-indene, and (c) a C14-indene.

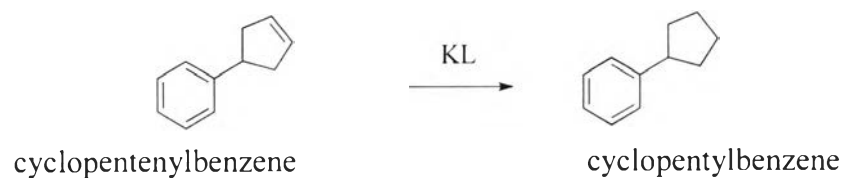
### 7.4.1.3 Confirmations of Changes in Hydrocarbon Species on KL

#### *Catalyst*

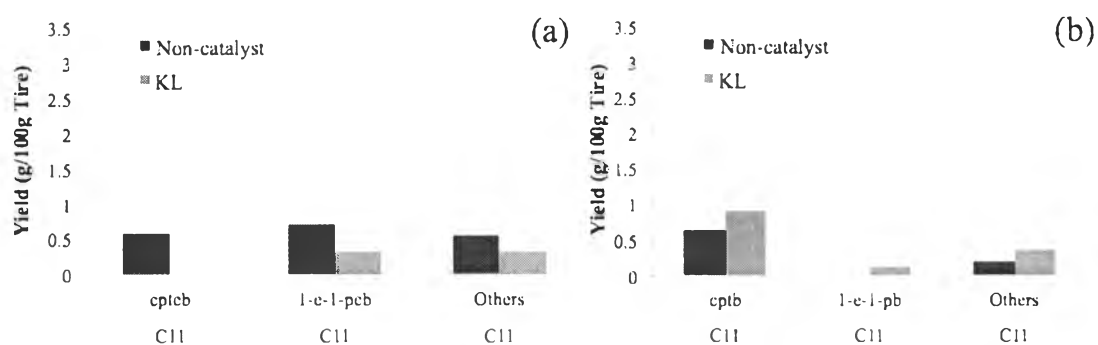
In the previous section, the GC x GC / TOF-MS results have revealed 7 hydrocarbon species that were changed upon the use of the KL catalyst. The changes of hydrocarbon species are confirmed in this section by using HSQC-NMR. Two chemical-shift (e.g.  $^1\text{H}$  and  $^{13}\text{C}$ ) databases of 7 hydrocarbon species that exist in pyrolysis oils as shown in Table 7.1 were employed for analysis. The chemical shifts were relevant to Sigma Aldrich  $^1\text{H}$  and  $^{13}\text{C}$  references (Pouchert and Behnke, 1993).

#### *(a) Changes of C11-Alkenylbenzenes to C11-Alkylbenzenes*

As observed from the GC x GC / TOF-MS results, the details on the changes of C11-alkenylbenzenes and C11-alkylbenzenes yields are shown in Figure 7.8 (a) and (b), respectively. The major component of C11-alkenylbenzenes is cyclopentenylbenzene (cpteb) ( $m/z = 144.110$ ) whose concentration decreases the most among the members in its group upon the use of KL. Likewise, among all C11-alkylbenzenes, cyclopentylbenzene (cptb) ( $m/z = 146.110$ ) is the member whose concentration increases significantly with using the KL catalyst. Cyclopentenylbenzene and cyclopentylbenzene are therefore representatives in their groups to investigate the changes of C11-alkenylbenzenes to C11-alkylbenzenes. With the findings observed above, it is proposed that an alkenylbenzene is hydrogenated by the KL catalyst to an alkylbenzene as shown in Equation (1a) as an example. Figure 7.9 shows the comparison of HSQC-NMR spectra of oils from the non-catalyst and KL batches, and it is found that the contents of cyclopentenylbenzene (the C-H positions of A1 and A2 as shown in Figure 7.9 (a)) decrease in conjunction with the increase in the content of cyclopentylbenzene (the C-H positions of B1 and B2 as shown in Figure 7.9 (b)).

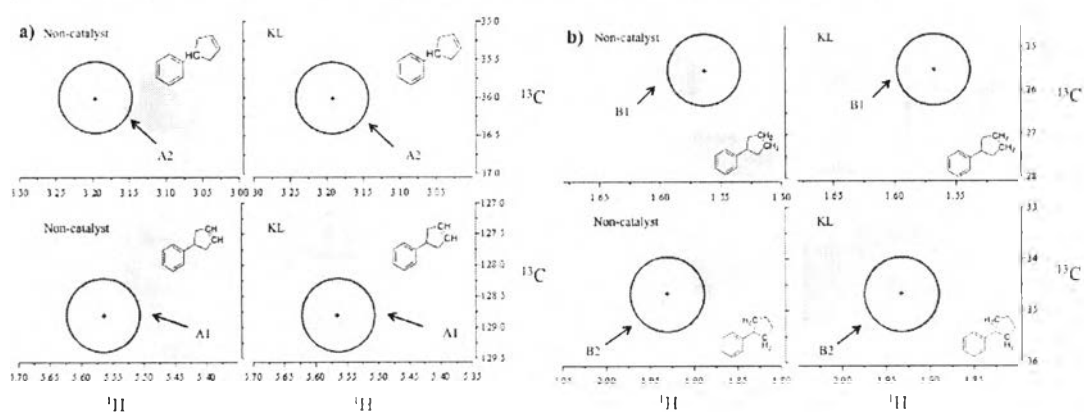


(1a)



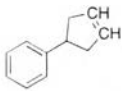
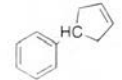
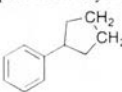
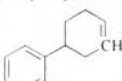
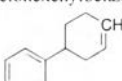
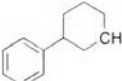
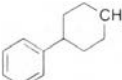
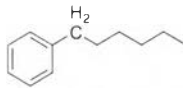
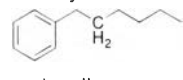
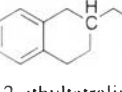
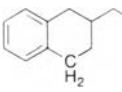
**Figure 7.8** Yields of members in (a)C11-alkenylbenzenes, and (b) C11-alkylbenzenes with using KL catalyst.

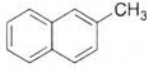
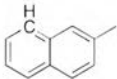
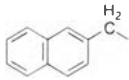
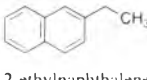
It can be concluded that the results from the HSQC-NMR are consistent with those observed from GC  $\times$  GC / TOF-MS. Therefore, Equation (1a) and the reaction pathway (a) in Figure 7.6 are proven to occur with using KL catalyst.



**Figure 7.9** HSQC-NMR spectra of assigned compounds: (a) cyclopentenylbenzene, and (b) cyclopentylbenzene in oils from non-catalyst (left) and KL (right) batches.

**Table 7.1**  $^1\text{H}$  and  $^{13}\text{C}$  NMR chemical shift of components in TDOs

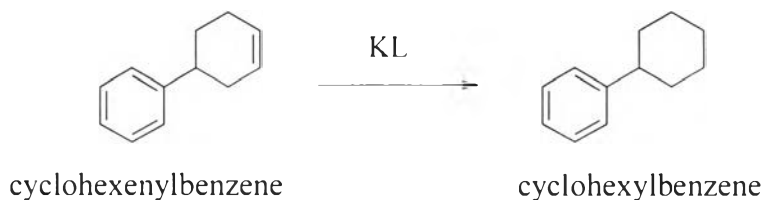
Group	Class	Carbon number	Assigned compound	$m/z$	Symbols	Chemical Shift		
						$^1\text{H}^a$	$^{13}\text{C}^b$	
MAHS	Alky/benzenes	11		144.110	A1	5.56	128.6	
			cyclopent-3-en-1-ylbenzene		A2	3.18	36.1	
					B1	1.56	25.5	
		cyclopentylbenzene		B2	1.93	34.6		
								
		cyclopentylbenzene						
	Alky/benzenes	12		158.110	C1	5.59	126	
			cyclohexenylbenzene		C2	5.59	128.3	
								
		cyclohexenylbenzene						
		Alkenyl/benzenes	12		160.110	D1	1.49	25.0
				cyclohexylbenzene		D2	1.53	25.4
								
cyclohexylbenzene								
Tetraolins	12		162.140	E1	2.72	36.0		
		hexylbenzene		E2	1.57	31.4		
								
		hexylbenzene						
			160.125	F1	1.57	37.0		
		2-ethyltetralin		F2	2.9	28.8		
								
2-ethyltetralin								

Group	Class	Carbon number	Assigned compound	$m/z$	Symbols	Chemical Shift	
						$^1\text{H}^a$	$^{13}\text{C}^b$
DAHs		11	 2-methylnaphthalene	142.080	G1	2.63	19.4
			 2-methylnaphthalene		G2	8.18	125.5
		12	 2-ethylnaphthalene	156.094	H1	2.71	26.6
			 2-ethylnaphthalene		H2	1.13	14.5

<sup>a,b</sup> Due to the complexity of components in TDOs, the chemical shift of  $^1\text{H}$  and  $^{13}\text{C}$  may occur in range of  $\pm 0.1$  for  $^1\text{H}$  and  $\pm 1.0$  for  $^{13}\text{C}$ . The chemical shift of each compounds were attributed from Aldrich chemical reference. (Pouchert and Behnke, 1993)

*(b) Conversion of C12-Alkenylbenzenes to C12-Alkylbenzenes*

The most relevant C12 species in alkenylbenzenes (alke) is cyclohexenylbenzene (chxeb) ( $m/z = 158.110$ ), and those of C12 alkylbenzenes is cyclohexylbenzene (chxb) ( $m/z = 160.125$ ) as listed in Table 7.1. From Figure 7.10(a), the yield of cyclohexenylbenzene (chxeb) decreases while cyclohexylbenzene (chxb) increase. The results indicate that the KL catalyst can provide hydrogenation on cyclohexenylbenzene, to form cyclohexylbenzene as shown in Equation (2a).



(2a)

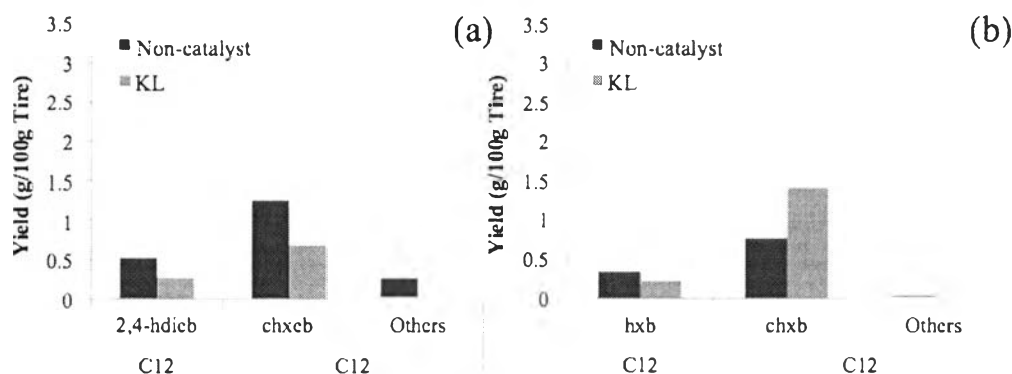


**Figure 7.10** (a) Yield of members in C12-alkenylbenzenes, and (b) Yields of members in C12-alkylbenzenes with using KL catalyst.

Figure 7.11 shows the comparison of HSQC-NMR spectra of oils from non-catalyst and KL batches, and it is found that the contents of cyclohexenylbenzene, the C-H positions of C1 and C2 as shown in Figure 7.11 (a), decrease in conjunction with the increase in the content of cyclohexylbenzene at G1 and G2 C-H positions as shown in Figure 7.11 (b). Therefore, the results from HSQC-NMR are consistent with those observed from GC  $\times$  GC / TOF-MS. Therefore, the reaction pathway (b) in Figure 7.6 and Equation (1a) are confirmed to occur with using KL catalyst.

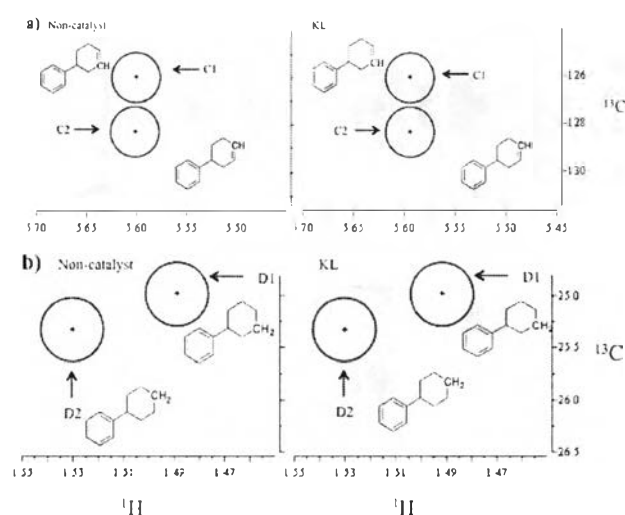
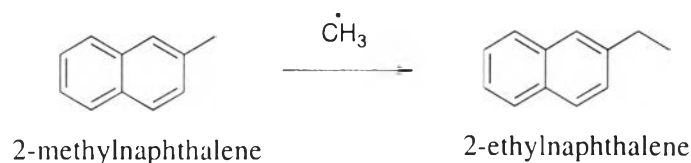


**Figure 7.11** HSQC-NMR spectra of assigned compounds: (a) cyclohexenylbenzene, and (b) cyclohexylbenzene in oil from non-catalyst (left) and KL (right) batches.



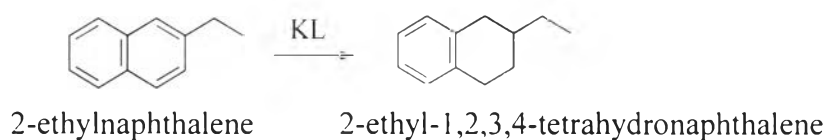
(c) Conversion of C12-DAHs to C12-Tetralins

Interestingly, the increment of MAHs, especially 1,2,3,4-tetrahydronaphthalenes (C12-tetralins), is found to be attributed from the conversion of C11- and C12-DAHs as supported by the significant decreases in the yields of DAHs (C11 and C12) as KL catalyst is used. The representative of C11-DAHs is 2-methylnaphthalene and C12-DAHs is 2-ethylnaphthalene ( $m/z = 156.094$ ), respectively, whose concentrations significantly decrease in conjunction with the dramatically increase in 2-ethyl-1,2,3,4-tetrahydronaphthalene (2-ethyltetralin) as shown in Figure 7.12. It is proposed that the 2-methylnaphthalene is first reacted with a methyl radical to give 2-ethylnaphthalene, as depicted in Equation (3a) and supported by the decreased yields of methane and ethane with using KL catalyst as shown in Figure 7.13.



(3a)

Subsequently, 2-ethylnaphthalene and ethylnaphthalene are hydrogenated by the KL catalyst to 2-ethyl-1,2,3,4-tetrahydronaphthalene as depicted in Equation (3b).



(3b)

The reason why methylnaphthalene can undergo methyl radical addition (Equation (3a)) is because the dehydrogenation of 2-ethylnaphthalene (Equation (3b)) is favoured with using KL catalyst, and behaves as a driving force.

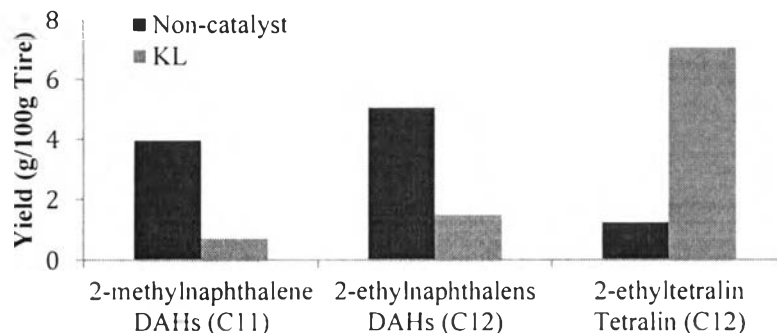


**Figure 7.12** Decreases in 2-methylnaphthalene and 2-ethylnaphthalene in conjunction with increase in 2-ethyltetralin.

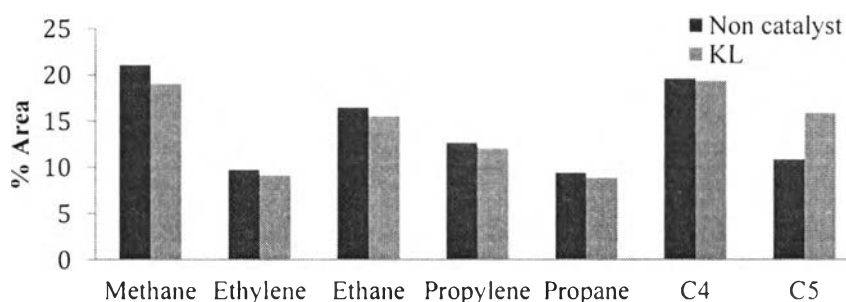


**Figure 7.13** Yield of gases obtained from using KL catalyst.

The existences of reaction in Equations (3a) and (3b) are supported by HSQC-NMR spectra in Figure 7.14. It is observed that the contents of 2-methylnaphthalene (C-H positions of G1 and G2 as shown in Figure 7.17 (a)) and 2-ethylnaphthalene (C-H positions of H1 and H2 as shown in Figure 7.17 (b)) decrease in conjunction with the increase in the content of 2-ethyl-1,2,3,4-tetrahydronaphthalene (2-ethyltetralin) (C-H position of F1 and F2 as shown in Figure 7.14 (c)). Evidently, the results from the HSQC-NMR are consistent with those of GC  $\times$  GC / TOF-MS; thus, Equations (3a) and (3b) and, as a result, the reaction pathways (c) and (d) in Figure 7.6 are proven to occur with using KL catalyst.

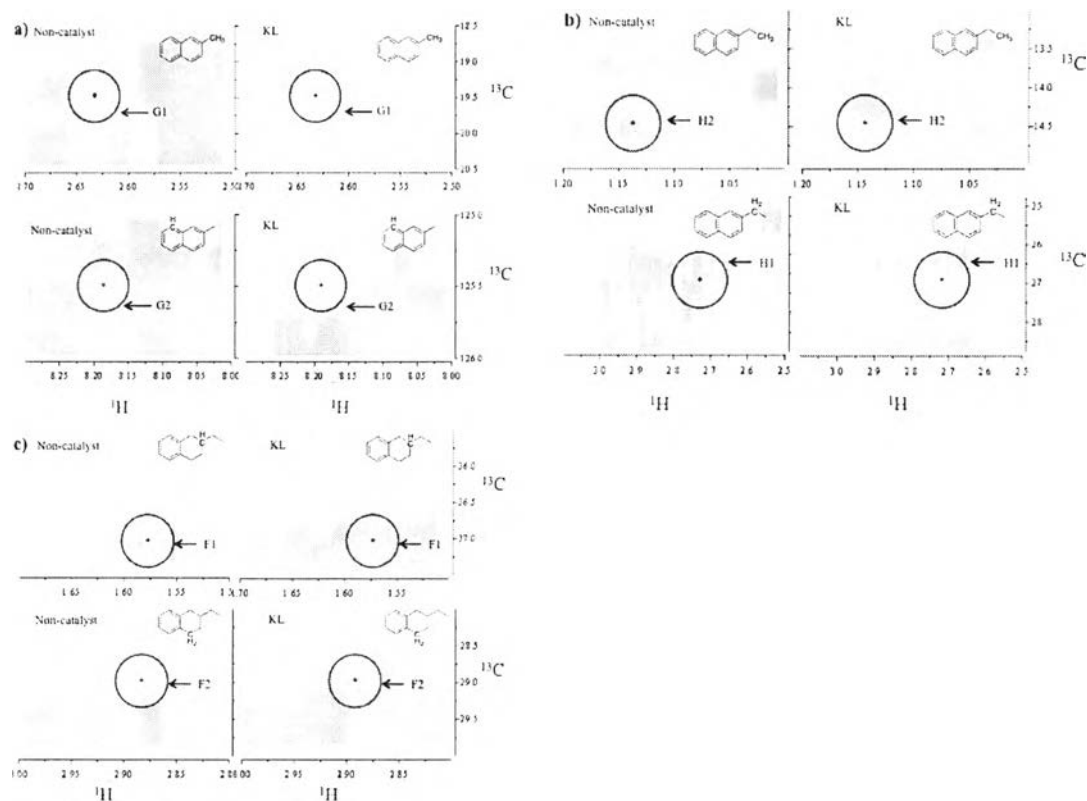


**Figure 7.14** HSQC-NMR spectra of assigned compounds: (a) 2-methylnaphthalene, (b) 2-ethylnaphthalene, and (c) 2-ethyltetralin in oils from non-catalyst (left) and KL (right) batches.

## 7.4.2 Influence of Rh on KL Catalyst

### 7.4.2.1 Changes of Components in TDO with Using Rh/KL

Figure 7.15 shows the changes of products components in TDOs with using Rh/KL catalyst, and it was found that the obvious changes are on MAHs and DAHs, whereas the SATs, PAHs, PPAHs, TERs, and OLEs do not show significantly change. Therefore, the surface activity of Rh/KL catalyst is observed based on the reaction pathways on Rh/KL catalyst as illustrated in Figure 7.16.

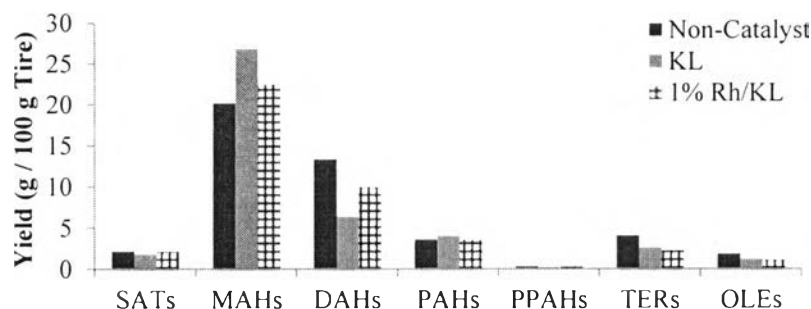


**Figure 7.15** Yield of hydrocarbon species in tire-derive oils from non-catalyst, KL, and Rh/KL batches.

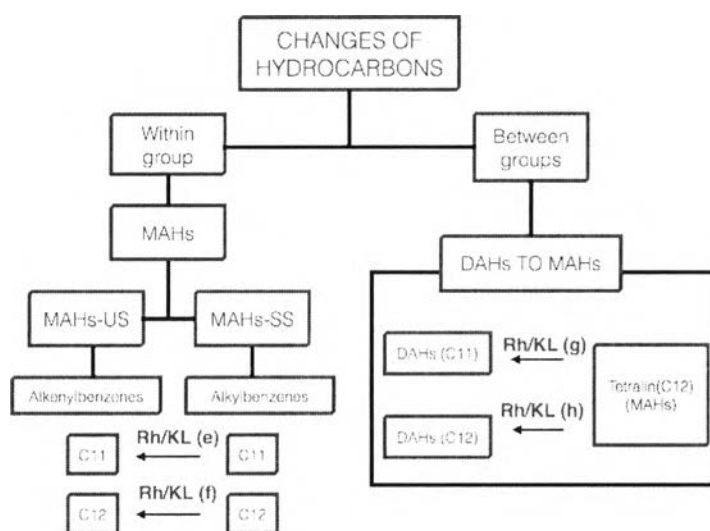


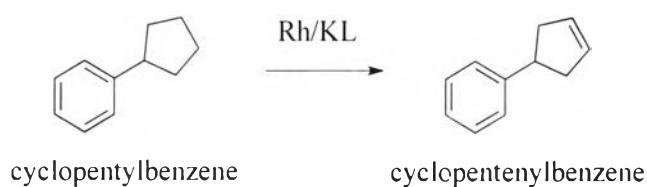
**Figure 7.16** Possible reaction pathways on Rh/KL.

#### 7.4.2.2 Possible reactions on Rh/KL

##### (a) Conversion of C11-Alkylbenzenes and C11-Alkenylbenzenes

In the previous sections, it was shown that the KL catalyst can provide hydrogenation of C11-alkenylbenzenes to C11-alkylbenzenes. When the Rh was introduced on the KL catalyst, the results show that C11-alkylbenzenes decrease in conjunction with the increase in C11-alkenylbenzenes as shown in Figure 7.17. The members of C11-alkylbenzenes are cyclopentylbenzene (cptb) and 1-ethyl-1-propylbenzene (1-e-1-pb), and those of C11-alkenylbenzenes are cyclopentenylbenzene and 1-ethyl-1-propylbenzene, whose yields are shown in

Figure 7.18 (a) and (b), respectively. The significant changes in those species are observed together with the decrease of cyclopentylbenzene and the increases of cyclopentenylbenzene. With the findings observed above, it is proposed that cyclopentylbenzene is dehydrogenated by Rh/KL to cyclopentenylbenzene as illustrated in Equation (4a).



(4a)

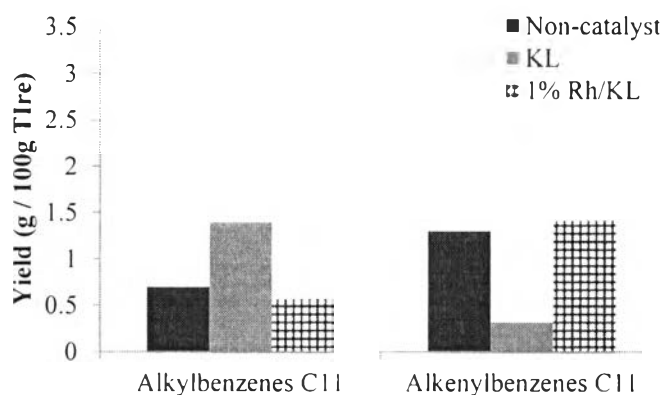


**Figure 7.17** Yields of C11-alkylbenzenes and C11-alkenylbenzenes with using non-catalyst, KL, and Rh/KL batches.

Figure 7.19 shows the comparison of HSQC-NMR spectra of oil from the KL and Rh/KL batches, and it is found that the contents of cyclopentylbenzene (the C-H positions of B1 and B2 as shown in Figure 7.18 (a)) decrease in conjunction with the increase in the contents of cyclopentenylbenzene (the C-H positions of A1 and A2 as shown in Figure 7.18 (b)). As a result, the results from the HSQC-NMR are consistent with those observed from GC  $\times$  GC / TOF-MS.

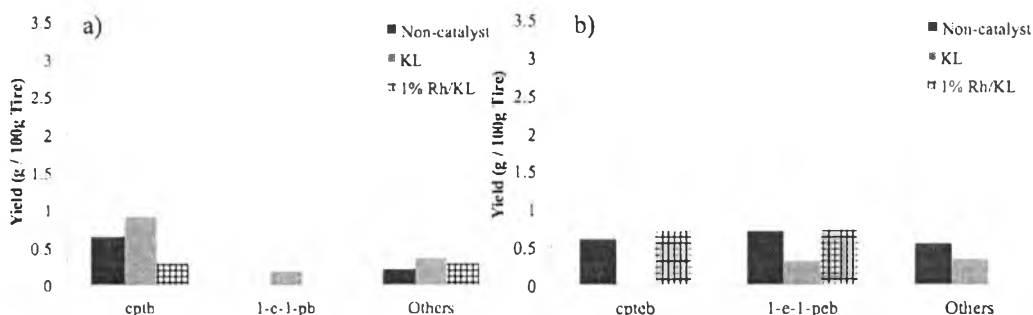


**Figure 7.18** (a) Yield of members in C11-alkylbenzenes, and (b) Yields of members in C11-alkenylbenzenes with using KL and Rh/KL catalysts.

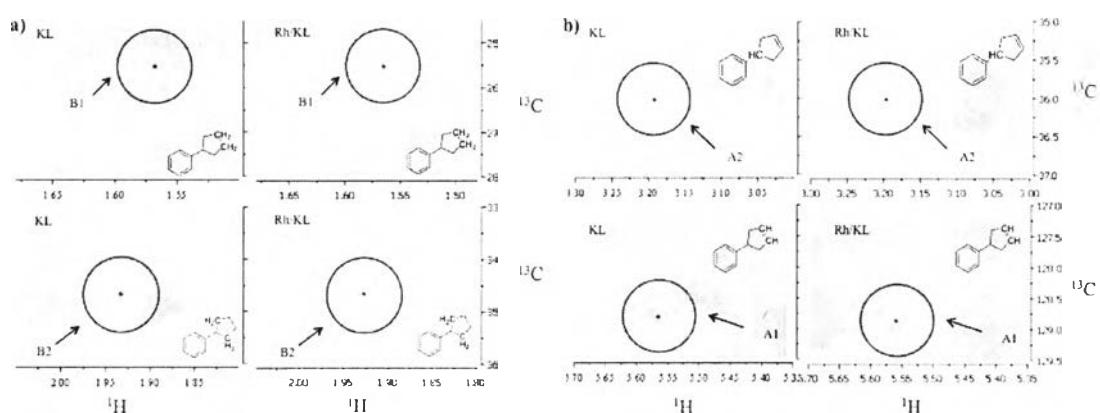


**Figure 7.19** HSQC-NMR spectra of assigned compounds: (a) cyclopentylbenzene, and (b) cyclopentenybenzene in oils from KL (left) and Rh/KL (right) batches.

Therefore, Equation (4a) and the reaction pathway (e) in Figure 7.16 are proven to occur with using Rh/KL catalyst. According to the results, it can be concluded that Rh provides dehydrogenation of C11-alkylbenzenes to C11-alkenylbenzenes.

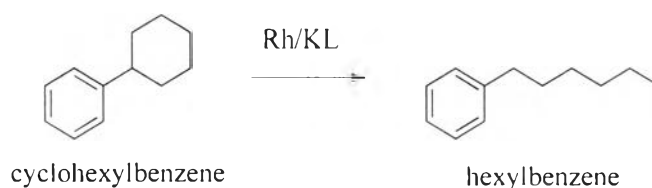
#### (b) Conversion of C12-Alkylbenzenes and C12-Alkenylbenzenes

In the previous sections it was shown that the KL catalyst can provide hydrogenation of C12-alkenylbenzenes to C12-alkylbenzenes. When the Rh was introduced on the KL catalyst, the results show that the C12-alkylbenzenes and C12-alkenylbenzenes do not significantly change as shown in Figure 7.20. The numbers of C12-alkylbenzenes are cyclohexyllbenzene (chxb) and hexylbenzene (hxb), and the numbers of C12-alkenylbenzenes are cyclohexenylbenzene (chexb)

and 3-hexenylbenzene (3-hxeb) as, whose yields are shown in Figure 7.21 (a) and (b), respectively. The cyclohexenylbenzene (chxeb) and 3-hexenylbenzene (3-hxeb) do not change upon the used of the Rh/KL catalyst, whereas the yields of cyclohexylbenzene (chxb) decreases in conjunction with the increase in the hexylbenzene (hxb) yield.

Two possible mechanisms that could take place on a metal surface have been proposed; that are, multiplet and dicarbene mechanisms (Gault *et al.*, 1981). Mutiplet mechanism occurs with molecules physically adsorbed at edgewise or interstitial sites on the metal surface. The bond is consequently stretched, and can be readily attacked by a chemisorbed hydrogen on the metal surface, leading to hydrogenolysis. Dicarbene mechanism usually occurs with unsaturated molecules. The chemisorption of an unsaturated hydrocarbon first takes place on a metal surface after the rupture of C-H bonds, and then the molecule is immediately bonded with the metal surface. Subsequently, the neighbor hydrogen atom is readily attacked via hydrogenolysis, and then the products desorb from the metal surface. For both mutiplet and dicarbene mechanisms, two adsorption modes, which are five-atom and six-atom adsorption modes, can be possible. Selective hydrogenolysis on a cyclic hydrocarbon is taken place at bisecondary C-C bond, which can be ruptured via six-atom adsorbtion mode whereas the five-atom adsorption mode leads to selective hydrogenolysis at secondary-tertiary C-C bond.

Therefore, it is proposed that the ring of cyclohexylbenzene is opened the ring through multiplet mechanism to give hexylbenzene as illustrated in Equation (5a).



(5a)

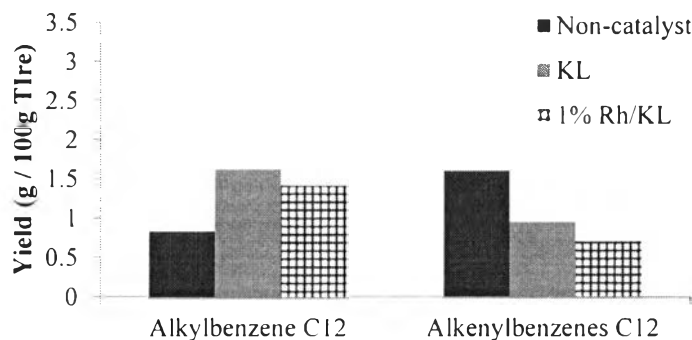


**Figure 7.20** Yields of alkylbenzenes (C12) and alkenylbenzenes (C12).

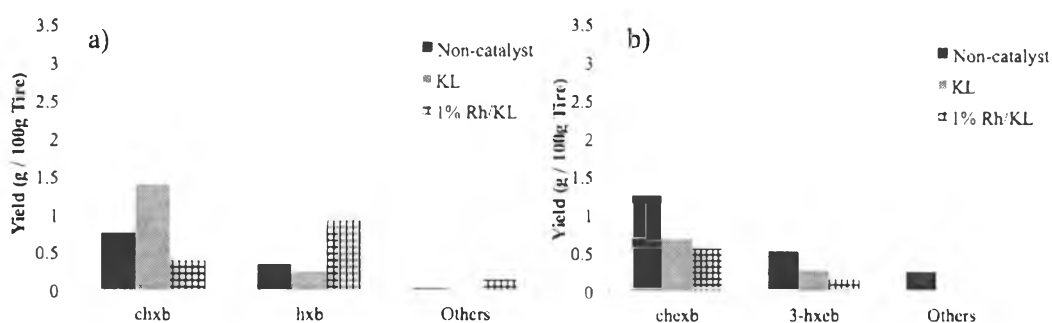


**Figure 7.21** Yields of members in (a) C12-alkylbenzenes, and (b) C12-alkenylbenzenes with using KL and Rh/KL catalysts.

Figure 7.22 shows the comparison of HSQC-NMR spectra of oils from the KL and Rh/KL batches, and it can be seen that the contents of cyclohexylbenzene (the C-H positions of D1 and D2 as shown in Figure 7.22 (a)) decrease in conjunction with the increase in the contents of hexylbenzene (the C-H positions of E1 and E2 as shown in Figure 7.22 (b)). Therefore, the results from the HSQC-NMR are consistent with those observed from GC  $\times$  GC / TOF-MS.



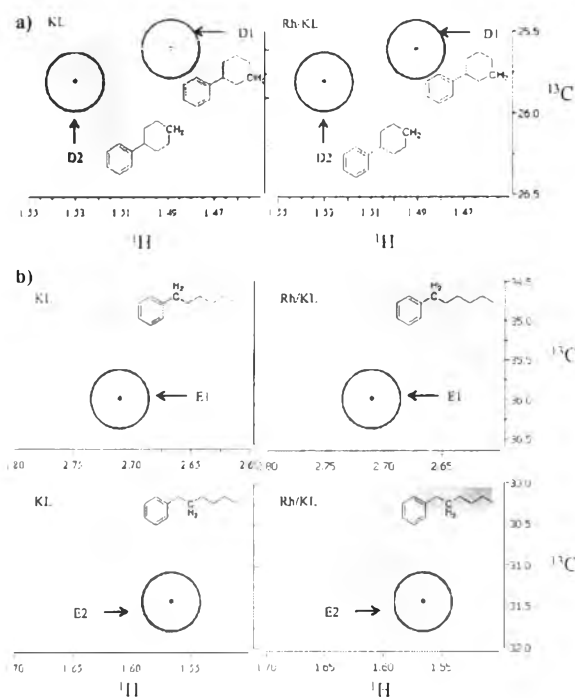
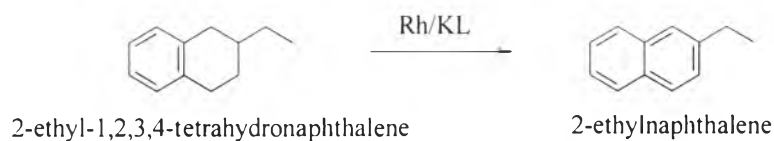


**Figure 7.22** HSQC-NMR spectra of assigned compounds: (a) cyclohexylbenzene, and (b) hexylbenzene in oils from KL (left) and Rh/KL (right) batches.

According to the results, it can be concluded that Rh drives ring opening of cyclohexylbenzene to hexylbenzene on the KL catalyst as shown in Equation (5a). The Rh/KL has no effect on C12-alkenylbenzenes, but selectively produces hexylbenzene in C12-alkylbenzenes when compared with non-catalyst batch. Therefore, the reaction pathway (f) in Figure 7.16 does not occur on the Rh/KL catalyst.

*(c) Conversion of C12-DAHs and C12-Tetralins*

The KL catalyst was found to hydrogenate 2-ethyl-naphthalene to 2-ethyl-1,2,3,4-tetrahydronaphthalene (2-ethyltetralin). When the Rh was introduced on the KL catalyst, the results show that 2-ethyl-1,2,3,4-tetrahydronaphthalene, as shown in Figure 7.23 (a), dramatically decreases in conjunction with the increase in 2-ethyl-naphthalene and 2-methylnaphthalene as shown in Figure 7.23 (b). It indicates that Rh can catalyze dehydrogenation of 2-ethyl-1,2,3,4-tetrahydronaphthalene (2-ethyltetralin) to 2-ethyl-naphthalene as depicted in Equation (6a).



(6a)

The increment of 2-ethylnaphthalene can be attributed from the decrement of 2-ethyl-1,2,3,4-tetrahydronaphthalene (2-ethyltetralin). Since the change of 2-methylnaphthalene is driven by the driving force of the hydrogenation of 2-ethylnaphthalene thus, when the Rh is introduced on the KL catalyst, 2-ethyl-1,2,3,4-tetrahydronaphthalene (2-ethyltetralin) was dehydrogenated. Therefore, the driving force for the conversion of 2-methylnaphthalene to 2-ethylnaphthalene also diminishes. As a result, the yield of 2-methylnaphthalene increases with using the Rh/KL catalyst. Nonetheless, some of 2-methylnaphthalene undergoes Equation (3a) since the decreases in yields of gases (e.g. methane and ethane) are observed as shown in Figure 7.24.

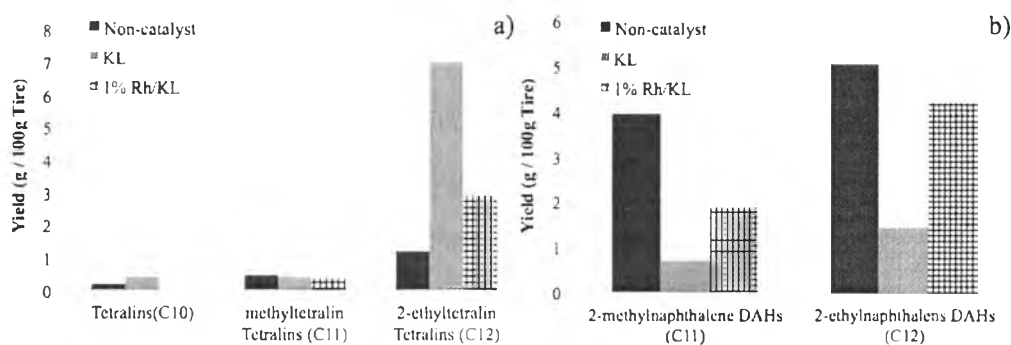


**Figure 7.23** Yields of members in (a) Tetralins, and (b) DAHs with using KL and Rh/KL catalysts.

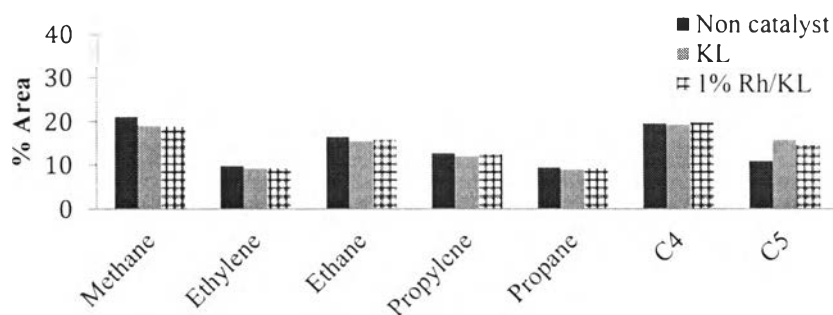


**Figure 7.24** Yield of gases obtained from used of KL and Rh/KL catalysts.

Figure 7.25 shows the comparison of HSQC-NMR spectra of oils from the KL and Rh/KL batches, and it is found that the contents of 2-ethyl-1,2,3,4-tetrahydronaphthalene (2-ethyltetralin) (the C-H positions of F1 and F2 as shown in Figure 7.28 (a)) decrease in conjunction with the increases in the contents of 2-methylnaphthalene (the C-H positions of H1 and H2 as shown in Figure 7.25 (b)) and the contents of 2-ethylnaphthalene (the C-H positions of G1 and G2 as shown in Figure 7.25 (c)). Therefore, the results from the HSQC-NMR are consistent with those observed from GC  $\times$  GC / TOF-MS. According to the results, it can be concluded that Rh over KL catalyst can dehydrogenate 2-ethyl-1,2,3,4-tetrahydronaphthalene (2-ethyltetralin) to 2-ethylnaphthalene. Therefore, Equation (6a) and reaction pathways (g) and (h) are proven to occur with using Rh/KL catalyst.

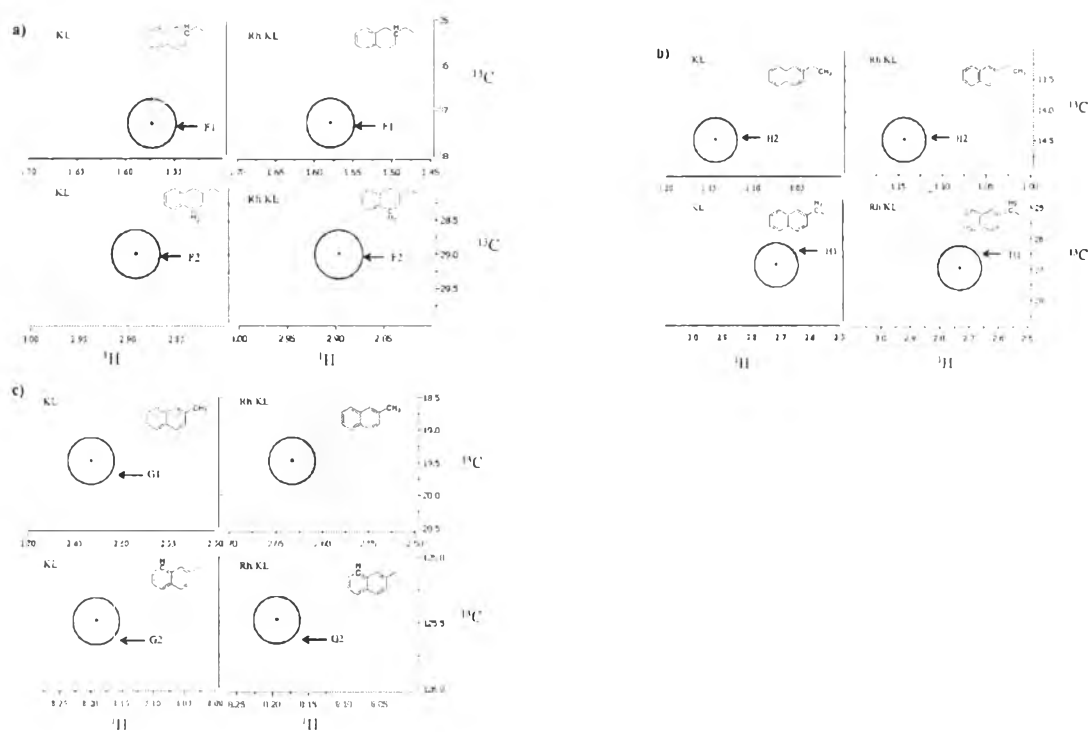


**Figure 7.25** HSQC-NMR spectra of assigned compounds: (a) 2-ethyltetralin, (b) 2-ethylnaphthalene, and (c) 2-methylnaphthalene in oils from KL (left) and Rh/KL (right) batches.

## 7.5 Conclusions

The activities on the surfaces of KL and Rh/KL have been elucidated, and it was found that the KL catalyst can provide hydrogenation of C11-alkenylbenzenes (mostly, cyclopentenylbenzene), C12-alkenylbenzenes (mostly, cyclohexenylbenzene), and DAHs(C12) (mostly, 2-ethylnaphthalene); moreover, rhodium can provide dehydrogenation of tetralins (C12) (mostly, 2-ethyltetralin), which is a species in MAHs, to C12-DAHs (mostly, 2-ethylnaphthalene). In addition, the Rh/KL catalyst can open the ring of cyclohexylbenzene via multiplet mechanism. As a result, Rh reduces hydrogenation ability of the KL catalyst. The reactions taken place on the KL and Rh/KL catalysts are summarized in Figure 7.26.

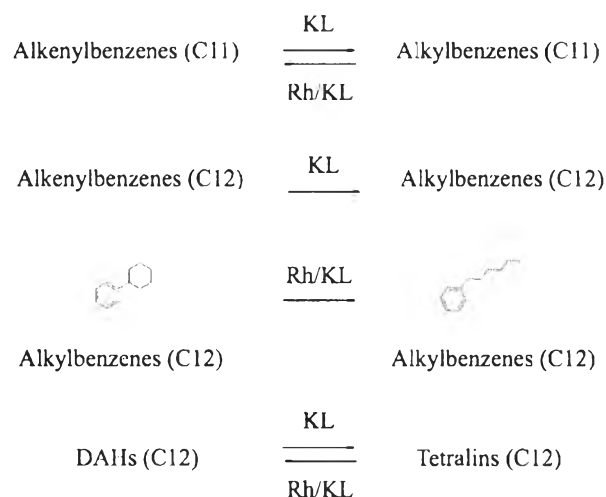


**Figure 7.26** Summary of reaction pathways on KL and Rh/KL.

## 7.6 Acknowledgements

The following agencies are acknowledged for their mutual financial support: The Thailand Research Fund (TRF) and Center of Excellence on Petrochemical and Materials Technology.

## 7.7 References

- Álvarez-Rodríguez, J.A., Guerrero-Ruiz, A., Rodríguez-Ramos, I., and Arcoya-Martín, A. (2005). Modifications of the citral hydrogenation selectivities over Ru/KL-zeolite catalysts induced by the metal precursors. *Catalysis Today*, 107–108, 302–309.
- Azzam, K.G., Jacobs, G., Shafer, W.D. and Davis, B.H. (2010). Aromatization of hexane over Pt/KL catalyst: Role of intracrystalline diffusion on catalyst performance using isotope labeling. *Journal of Catalysis*, 270(2), 242-248.
- Ben, H. and Ragauskas, A.J. (2011). Heteronuclear Single-Quantum Correlation–Nuclear Magnetic Resonance (HSQC–NMR) Fingerprint Analysis of Pyrolysis Oils. *Energy & Fuels*, 25(12), 5791-5801.
- Brown, C.A. (1973). Kalliation. I. Remarkable fast reaction of potassium hydride with amines and other feeble organic acids. Convenient rapid route to elusive new superbases. *Journal of the American Chemical Society*, 95(3), 982-983.
- David, K., Pu, Y., Foston, M., Muzzy, J. and Ragauskas, A. (2008). Cross-Polarization/Magic Angle Spinning (CP/MAS) <sup>13</sup>C Nuclear Magnetic Resonance (NMR) Analysis of Chars from Alkaline-Treated Pyrolyzed Softwood. *Energy & Fuels*, 23(1), 498-501.
- Dallüge, J., Vreuls, R.J.J., Beens, J. and Brinkman, U.A.T. (2002). Optimization and characterization of comprehensive two-dimensional gas chromatography with time-of-flight mass spectrometric detection (GC×GC–TOF MS). *Journal of Separation Science*, 25(4), 201-214.
- Dũng, N.A., Wongkasemjit, S. and Jitkarnka, S. (2009). Effects of pyrolysis temperature and Pt-loaded catalysts on polar-aromatic content in tire-derived oil. *Applied Catalysis B: Environmental*, 91(1–2), 300-307.
- Friedman, S., Kaufman, M.L. and Wender, I. (1971). Alkali metals as hydrogenation catalysts for aromatic molecules. *The Journal of Organic Chemistry*, 36(5), 694-697.
- Gault, F.G. (1981). Mechanisms of Skeletal Isomerization of Hydrocarbons on

- Metals. *Advances in Catalysis*. D.D. Eley, H.P. and Paul, B.W., Academic Press. Volume 30: 1-95.
- Jacquin, M., Jones, D.J., Rozière, J., Albertazzi, S., Vaccari, A., Lenarda, M., Storaro, L., and Ganzerla, R. (2003). Novel supported Rh, Pt, Ir and Ru mesoporousaluminosilicates as catalysts for the hydrogenation of naphthalene. *Applied Catalysis A: General*, 251, 131–141.
- Manzano, C., Hoh, E. and Simonich, S.L.M. (2012). Improved Separation of Complex Polycyclic Aromatic Hydrocarbon Mixtures Using Novel Column Combinations in GC × GC/ToF-MS. *Environmental Science & Technology*, 46(14), 7677-7684.
- McEnally, C.S. and Pfefferle, L.D. (2007). Improved sooting tendency measurements for aromatic hydrocarbons and their implications for naphthalene formation pathways. *Combustion and Flame*, 148(4), 210-222.
- Melbye, A.G., Brakstad, O.G., Hokstad, J.N., Gregersen, I.K., Hansen, B.H., Booth, A.M., Rowland, S.J. and Tollefsen, K.E. (2009). Chemical and toxicological characterization of an unresolved complex mixture-rich biodegraded crude oil. *Environmental Toxicology and Chemistry*, 28(9), 1815-1824.
- Nurunnabi, M., Fujimoto, K.I., Suzuki, K., Li, B., Kado, S., Kunimori, K., and Tomishige, K. (2006). Promoting effect of noble metals addition on activity and resistance to carbon deposition in oxidative steam reforming of methane over NiO–MgO solid solution. *Catalysis Communications*, 7, 73–78.
- Pines, H. and Eschinazi, H.E. (1955). Studies in the Terpene Series. XXIV.1 Sodium-catalyzed Double Bonds Migration and Dehydrogenation of d-Limonene, 1- $\alpha$ -Phellandrene and of 2,4(8)- and 3,8(9)-p-Menthadiene2,2a. *Journal of the American Chemical Society*. 77(23), 6314-6321.
- Pithakratanayothin, S. and Jitkarnka, S. (2014). Analysis of a tire-derived oil using GC × GC – TOF/MS for better identification and grouping of hydrocarbon compounds. *Proceeding of the 29<sup>th</sup> ICSW 2014, Philadelphia, USA*.

- Pouchert, C.J. and Behnke, J. The Aldrich Library of  $^{13}\text{C}$  and  $^1\text{H}$  FT-NMR Spectra, Aldrich Chemical, □ Milwaukee, WI, 1992, 4,300pp
- Sato, T., Kunimori, K., and Hayashi, S. (1999). Dynamics of benzene, cyclohexane and n-hexane in KL zeolite studied by  $^2\text{H}$  NMR. *Phys. Chem. Chem. Phys.*, 1(16), 3839-3843.
- Shukla, B., Miyoshi, A. and Koshi, M. (2010). Role of Methyl Radicals in the Growth of PAHs. *Journal of the American Society for Mass Spectrometry*, 21(4), 534-544.
- Slaugh, L.H. (1967). Metal hydrides. Hydrogenation and isomerization catalysts. *The Journal of Organic Chemistry*, 32(1), 108-113.
- Slaugh, L.H. (1968). Hydrogenation of benzene to phenylcyclohexane with supported alkali metal catalysts. *Tetrahedron*, 24(12), 4525-4533.
- Stapp, P.R. and Kleinschmidt, R.F. (1965). The Isomerization of Cyclooctadienes to cis-Bicyclo[3.3.0]oct-2-ene. *The Journal of Organic Chemistry*, 30(9), 3006-3009.
- Williams, P.T., Besler, S. and Taylor, D.T. (1990). The pyrolysis of scrap automotive tyres: The influence of temperature and heating rate on product composition. *Fuel*, 69(12), 1474-1482.
- Williams, P.T. and Besler, S. (1995). Pyrolysis-thermogravimetric analysis of tyres and tyre components. *Fuel*, 74(9), 1277-1283.
- Williams, P.T. and Bottrill, R.P. (1995). Sulfur-polycyclic aromatic hydrocarbons in tyre pyrolysis oil. *Fuel*, 74(5), 736-742.
- Williams, P.T. and Nazzari, J.M. (1995). Polycyclic aromatic compounds in oils derived from the fluidised bed pyrolysis of oil shale. *Journal of Analytical and Applied Pyrolysis*, 35(2), 181-197.